

Accepted Manuscript

Binding of triazole-linked galactosyl arylsulfonamides to galectin-3 affects *Trypanosoma cruzi* cell invasion

Marcelo Fiori Marchiori, Thalita B. Riul, Leandro Oliveira Bortot, Peterson Andrade, Getúlio G. Junqueira, Giuseppina Foca, Nunzianna Doti, Menotti Ruvo, Marcelo Dias-Baruffi, Ivone Carvalho, Vanessa Leiria Campo

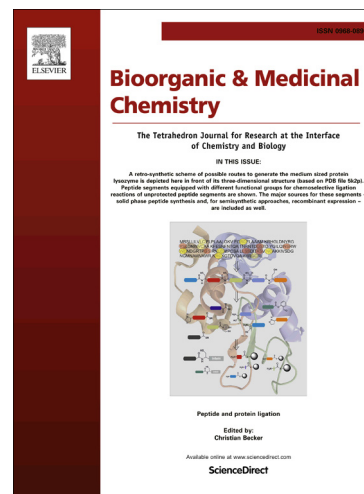
PII: S0968-0896(17)31366-4
DOI: <https://doi.org/10.1016/j.bmc.2017.09.042>
Reference: BMC 14002

To appear in: *Bioorganic & Medicinal Chemistry*

Received Date: 4 July 2017
Revised Date: 22 September 2017
Accepted Date: 29 September 2017

Please cite this article as: Marchiori, M.F., Riul, T.B., Oliveira Bortot, L., Andrade, P., Junqueira, G.G., Foca, G., Doti, N., Ruvo, M., Dias-Baruffi, M., Carvalho, I., Campo, V.L., Binding of triazole-linked galactosyl arylsulfonamides to galectin-3 affects *Trypanosoma cruzi* cell invasion, *Bioorganic & Medicinal Chemistry* (2017), doi: <https://doi.org/10.1016/j.bmc.2017.09.042>

This is a PDF file of an unedited manuscript that has been accepted for publication. As a service to our customers we are providing this early version of the manuscript. The manuscript will undergo copyediting, typesetting, and review of the resulting proof before it is published in its final form. Please note that during the production process errors may be discovered which could affect the content, and all legal disclaimers that apply to the journal pertain.



Binding of triazole-linked galactosyl arylsulfonamides to galectin-3 affects *Trypanosoma cruzi* cell invasion

Marcelo Fiori Marchiori¹, Thalita B. Riul¹, Leandro Oliveira Bortot¹, Peterson Andrade¹, Getúlio G. Junqueira¹, Giuseppina Foca², Nunzianna Doti², Menotti Ruvo², Marcelo Dias-Baruffi¹, Ivone Carvalho¹, Vanessa Leiria Campo¹

1. Faculty of Pharmaceutical Sciences of Ribeirão Preto - USP. Av. do Café S/N, CEP 14040-903, Ribeirão Preto - SP, Brazil.

2. Istituto di Biostrutture e Bioimmagini, CNR, via Mezzocannone, 16, I-80134, Napoli.

vlcampo@fcfrp.usp.br

Abstract

The synthesis of the O-3 triazole-linked galactosyl arylsulfonamides **1-7** as potential inhibitors of *Trypanosoma cruzi* cell invasion is described. These target compounds were synthesized by Cu(I)-catalysed azide-alkyne cycloaddition reaction ('click chemistry') between different azide arylsulfonamides and the alkyne-based sugar 3-O-propynyl- β GalOMe. Inhibition assays of *T. cruzi* cell invasion with compounds **1-7** showed reduced values of infection index (~ 20) for compounds **3** and **5**, bearing the corresponding 5-methylisoxazole and 2,4-dimethoxypyrimidine groups, which also presented higher binding affinities to galectin-3 (EC_{50} 17-18 μ M) in Corning Epic label-free assays. In agreement with experimental results, the assessment of the theoretical binding of compounds **1-7** to galectin-3 by MM/PBSA method displayed higher affinities for compounds **3** (-9.7 Kcal/mol) and **5** (-11.1 Kcal/mol). Overall, these achievements highlight compounds **3** and **5** as potential *T. cruzi* cell invasion blockers by means of a galectin-3 binding-related mechanism, revealing galectin-3 as an important host target for design of novel anti-trypanosomal agents.

Keywords

Triazole, Galactosyl arylsulfonamides, "Click Chemistry", *Trypanosoma cruzi*, Cell invasion, Galectin-3, *trans*-Sialidase

1. Introduction

¹ Corresponding author. Tel.: +55 16 33154285; fax: +55 16 33154879; e-mail: vlcampo@fcfrp.usp.br

Chagas disease is among the most prevalent neglected tropical diseases, affecting an estimated 6 to 7 million people mostly with low socioeconomic status. Although this disease is endemic in Latin America, it is spreading as a worldwide threat due to globalization and population mobility to North America, Europe and others areas where it is non-endemic.^{1,2} Chagas disease is mainly transmitted by triatomine bugs that carry the protozoan parasite *Trypanosoma cruzi*, and make its eradication exceptionally difficult; furthermore, due to parasite's efficient ways of evading the host immune system, vaccination remains as a great challenge.^{2,3} Thus, the use of anti-trypanosomatid drugs is the unique choice for treatment and still relies only on benznidazole and nifurtimox, drugs with poor efficacy in chronic infection phase and recognized toxicity.³ In this regard, development of multi-target drug candidates able to block parasite invasion in the early stages of infection may represent an effective strategy against this neglected disease.

T. cruzi adhesion and invasion into host cells are regulated by complex interactions among parasite cell surface components, such as *trans*-sialidase (TcTS),⁴ mucins⁵ and cruzipain,⁶ as well as galectins-3 and -1,^{7,8} and Toll-like receptors present in host cells.^{9,3} *T. cruzi trans*-sialidase is anchored to the parasite membrane by glycosylphosphatidylinositol (GPI) and has a fundamental role on *T. cruzi* invasion since it catalyses the transfer of sialic acid from host glycoconjugates to β -galactopyranosyl acceptor groups on *T. cruzi* mucins.^{4,10-12} This transglycosylation reaction enables the parasite to be recognized by host cells and protects it against complement-independent lyses induced by human anti- α -galactosyl antibodies due to the generated negatively charged sialylated barrier.^{13,14} In addition, TcTS may induce the early escape of *T. cruzi* from lysosome-enriched parasitophorous vacuole (PV) formed in the host cell by removing sialic acid from lysosome-associated membrane glycoproteins (LAMP), followed by disruption of PV membranes with the aid of a parasite trypsin sensitive enzyme (TcTox).¹⁵ In turn, *T. cruzi* mucins (TcMUC) are also GPI anchored plasma membrane glycoproteins (about 60% carbohydrate by weight) highly expressed on *T. cruzi* surface, with about 2×10^6 copies per parasite. TcMUC play a significant role in the

parasite recognition process and invasion of host cells based on its acceptor substrate preferences for sialic acid, transferred by TcTS.^{16,17}

On the other hand, galectin-3 is a carbohydrate-binding lectin found in different host cell compartments that is also importantly involved in *T. cruzi* infection. It contains a conserved carbohydrate recognition domain (CRD) with affinity for β -galactosides containing glycoconjugates and acts as one of the receptors that mediates the adhesion of the parasite to the host cells, besides being involved in cell invasion and intracellular trafficking of the parasite.^{3,7,18} Galectin-3 is able to interact effectively with both *T. cruzi* surface mucins and laminin present in the extracellular matrix, establishing thus a bridge between these two components, which increases the recruitment of trypomastigotes to the extracellular matrix and their adhesion to cells.¹⁸ Galectin-3 can also act as marker of the cell biology events in *T. cruzi* infection, since it is able to interact with lysosome-associated membrane glycoproteins (LAMP) of macrophage cell phagosomes, accumulating around *T. cruzi* parasites that lysed the parasitophorous vacuole during the host cell infection.¹⁹

Novel compounds from distinct chemical classes have been recently reported as antitrypanosomal agents.²⁰⁻²⁸ For instance, potent trypanocidal activities have been described for tetrahydroquinoline-sulfonamide derivatives against epimastigote forms (Y strain) (**I**,²⁵ IC₅₀ 11.4 μ M and **II**,²⁶ IC₅₀ 31.7 μ M) (Fig. 1A), as well as strong inhibitory activity towards TcTS by chalcone-derived sulfonamides (**III**,²⁷ IC₅₀ 0.6 μ M) (Fig. 1B). In addition, a series of seven galactosyl-triazolo-benzenesulfonamides comprising β -galactosyl unit anomeric-linked to distinct arylsulfonamides via triazole ring was reported by Carvalho et al.,²⁸ being verified significant trypanocidal activity against trypomastigote forms (Tulahuen strain) for the 2,4-dimethoxypyrimidine-derivative **IV** (IC₅₀ 44.0 μ M), and strong inhibition against TcTS for the pyridine-derivative **V** (81% at 1 mM) (Fig. 1C). Differently from this series containing anomeric triazole-substituted galactosyl sugar, we had described the synthesis of 1,2,3-triazole amino acids-derived-3-O-galactosides as galectin-3 inhibitors, based on the known potential of O-3 triazole-galactose analogs to interact with galectin-3 CRD. High binding affinities for galectin-3 were

verified for Phe (**VI**)/ Lys (**VII**)-derived-3-O-galactosides (Fig. 1D), with corresponding K_D values of 7.8 μM and 4.6 μM .²⁹

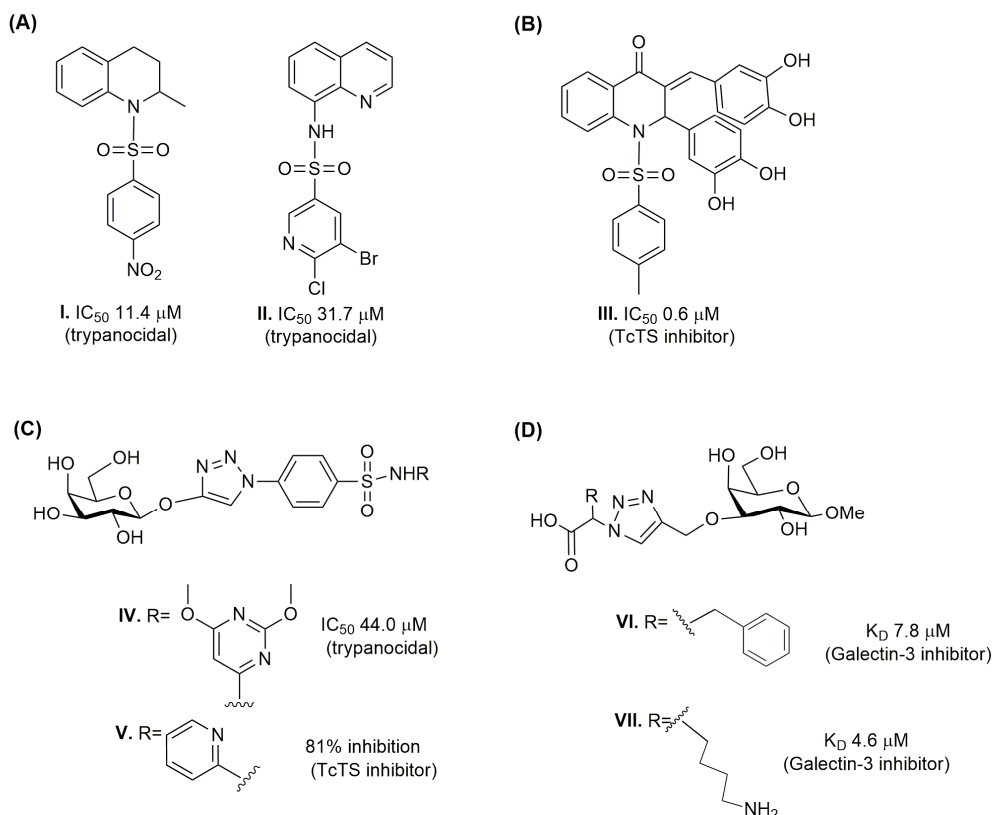


Figure 1. Representative compounds with significant trypanocidal effect (**I**, **II** and **IV**), and inhibitory activities against TcTS (**III** and **V**) and galectin-3 (**VI** and **VII**).

All these findings led us to postulate that novel hybrid glycoconjugates represented by 1,2,3-triazole arylsulfonamides-derived-3-O-galactosides, such as **1-7** (Fig. 2), may hamper *T. cruzi* cell invasion by possible dual inhibition of TcTS and galectin-3. Therefore, here we describe the synthesis of O-3 triazole-linked galactosyl arylsulfonamides **1-7**, via microwave-assisted Cu(I) 1,3-dipolar azide-alkyne cycloaddition (CuAAC), along with their evaluation on *T. cruzi* cell invasion process and inhibition of both TcTS and galectin-3.

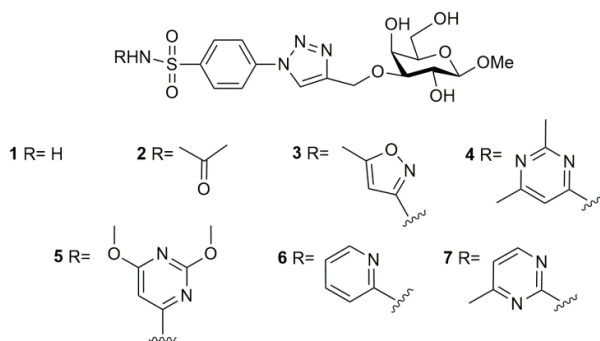


Figure 2. Chemical structures of the target triazole-linked galactosyl arylsulfonamides **1-7**.

2. RESULTS AND DISCUSSION

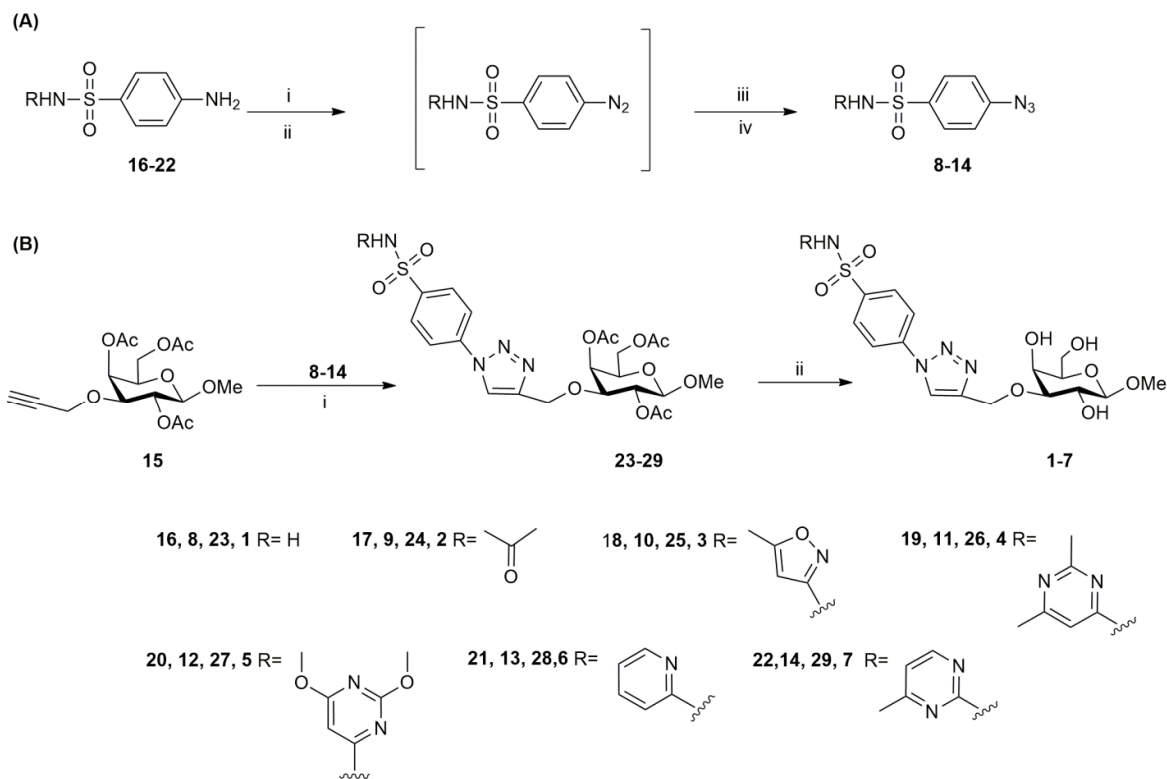
2.1. Synthesis

The syntheses of the O-3 triazole-linked galactosyl arylsulfonamides **1-7** by CuAAC required the previous preparation of the azide-arylsulfonamides **8-14**²⁸ and the alkyne-based sugar 3-O-propynyl- β GalOMe **15**²⁹ (Scheme 1) as their direct precursors.

Starting from the commercially available arylsulfonamides, named sulfanilamide **16**, sulfacetamide **17**, sulfamethoxazole **18**, sulfamethazine **19**, sulfadimethoxine **20**, sulfapyridine **21** and sulfamerazine **22**, the preparation of their corresponding azide arylsulfonamides **9-15** was firstly attempted by the treatment of **16-22** with *tert*-butyl nitrite and sodium azide under microwave irradiation.²⁸ However, the desired products **8-14** were obtained in very low yields (10-30%), possibly due to poor solubility of most precursors in the tested solvents (DMF, acetonitrile, dioxane and THF).³¹ To circumvent this limiting factor, we applied an alternative method based on the previous protonation of free 4-aminoaryl groups of **16-22**, turning them water-soluble and thus allowing the use of common NaNO_2 reagent for diazotation reaction (Scheme 1A).³² Therefore, treatment of **16-22** with aqueous sulfuric acid solution 17% (v/v), followed by dropwise addition of NaNO_2 solution for few minutes, led to diazo intermediates, which were subsequently treated with solid urea and NaN_3 (Scheme 1A). The ongoing formation of the azide derivatives **8-14** was indicated by their decreasing solubility until complete precipitation in the reaction mixture. After filtration, the products **8-14** were obtained in yields varying from 38% to 91%, being their

structures confirmed by ^1H NMR and IR [2100 cm^{-1} (N_3)].²⁸ Then, the alkyne-based sugar 3-O-propynyl- β GalOMe **15** was synthesized from commercial β GalOMe, under our previously described method applied to α GalOMe, giving **15** in 70% yield.³⁰ The ^1H NMR of **15** showed a characteristic doublet of H-1 at δ 4.15 (J 7.8 Hz), confirming its β configuration.

Once the azide-arylsulfonamides **8-14** and alkyne-functionalized **15** precursors were obtained, the syntheses of O-3 triazole-linked galactosyl arylsulfonamides **1-7** were carried out by Cu(I)-assisted 1,3-dipolar azide-alkyne cycloaddition reactions (CuAAC), in a microwave reactor utilizing the catalytic system CuSO_4 /sodium ascorbate and DMF as solvent.^{29,30,33} Thus, the peracetylated triazole-derivatives **23-29** were obtained after 30 min. of microwave irradiation at 100°C (150W), with regioselective formation of 1,4-disubstituted triazoles (Scheme 1B), in satisfactory yields varying from 60 to 70% after purification by column chromatography, except for compound **27** (47%), possibly due to the influence of the bulkier 4,6-dimethoxypyrimidine group on the CuAAC reaction. The structures of compounds **23-29** were confirmed by ^1H NMR analysis, which showed a characteristic singlet of *CH*-triazole around δ 8.0, signals of sugar at δ 4.9 (H-1), δ 3.3 (OCH_3) and δ 2.11-2.06 (OCOCH_3), as well as CH aromatic signals of arylsulfonamides at δ 8.4-7.8. Finally, compounds **23-29** were submitted to deacetylation reactions using 1 M NaOMe in MeOH,²⁹ affording the final triazole-linked galactosyl arylsulfonamides **1-7** (63-100%) after purification by column chromatography. (Scheme 1B).



Scheme 1. (A) Syntheses of azide-arylsulfonamides **8-14** precursors from the commercial arylsulfonamides **16-22**. Reagents and conditions: i. $\text{H}_2\text{SO}_4/\text{H}_2\text{O}$, 0°C ; ii. $\text{NaNO}_2/\text{H}_2\text{O}$, rt.; iii. $(\text{NH}_2)_2\text{CO}$, NaN_3 , H_2O , rt. (B) Syntheses of 1,2,3-triazole-linked galactosyl arylsulfonamides **1-7**. Reagents and conditions: i. Na ascorbate, CuSO_4 , DMF, microwave heating (100°C , 15 min); ii. NaOMe, MeOH, rt.

2.2. Biological assays

2.2.1. Inhibition of *T. cruzi* cell invasion

The capacity of compounds **1-7** to block invasion of fibroblasts cells (LLCMK2- monkey kidney epithelial cells) by *T. cruzi* trypomastigotes (Y strain) was evaluated by treatment of pre-formed adhered cells in circular coverslips with compounds **1-7** ($250\ \mu\text{M}$), followed by addition of trypomastigotes (1×10^5) after 30 min of contacting of the compounds with cells. After the incubation of the cultures for 18 h, the coverslips were fixed and stained for measuring the level of cell infection.^{34,35}

Firstly, it was observed a reduction in the percentage of infected fibroblasts treated with compounds **3** and **5**, bearing the corresponding 5-methylisoxazole and 2,4-dimethoxypyrimidine groups, with decreased values of 41% and 38%, respectively, if compared to 63% observed for non-treated cells, while the other tested compounds varied from 47% to 54% (Fig. 3A). In addition, compounds **3** and **5** also showed a significant reduction in the mean number of amastigotes within each cell, presenting 0.49 parasite/cell *versus* 1.0 for non-treated cells and a range of 0.81 to 0.61 for the remaining compounds (Fig. 3B). Lastly, the infection index values, obtained by multiplying the percentage of infected cells by the mean number of amastigotes per cell, were also determined for compounds **1-7**. It was verified a reduced infection index of about 20 for both compounds **3** and **5** *versus* 68 for the control without treatment. The infection index for the other tested compounds ranged from 44 to 28 (Fig. 3C).

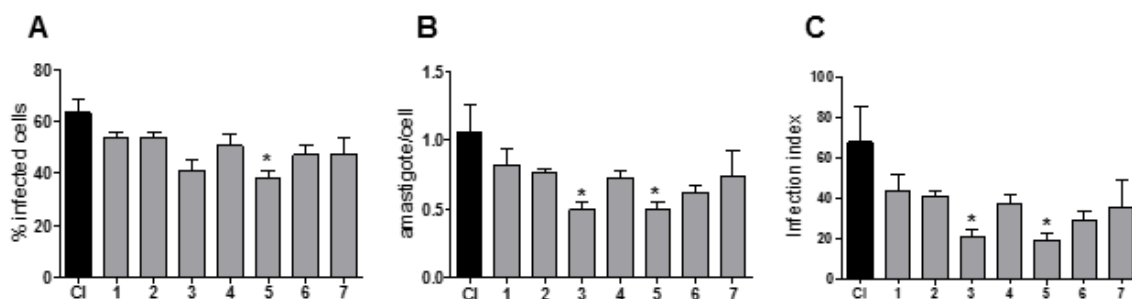


Figure 3. Inhibition of *T. cruzi* cell invasion by compounds **1-7**. (A) Percentage of infected fibroblasts; (B) Mean number of parasites (amastigotes) per cell; (C) Infection index assessed by optical microscopy after 18-hours treatment. * represents $p < 0.05$ of treated cells when compared to control (only medium) of a triplicate representative experiment; Cl-control.

Subsequently, we also investigated the cytotoxicity of compounds **1-7** in LLCMK2 fibroblasts as well as their direct trypanocidal effect, using the corresponding colorimetric MTT and resazurin-based methods as indicators of cell metabolic activity.³⁶ At the tested concentrations, none of the compounds were toxic for fibroblasts (67.5-500 μ M) or *T. cruzi* tripomastigote forms (31.25-250

μM), as shown in Fig. 4. Thus, since no trypanocidal effect was observed for compounds **1-7**, we may say that it has no correlation with the observed blocking of *T. cruzi* cell invasion.

Therefore, the satisfactory capacities of the tested compounds, remarkably **3** and **5**, to block *T. cruzi* invasion towards fibroblasts cells, prompted us to investigate their inhibitory activities against *T. cruzi* trans-sialidase (TcTS) and galectin-3 found in host cells, since they are essential targets involved in *T. cruzi* cell invasion.

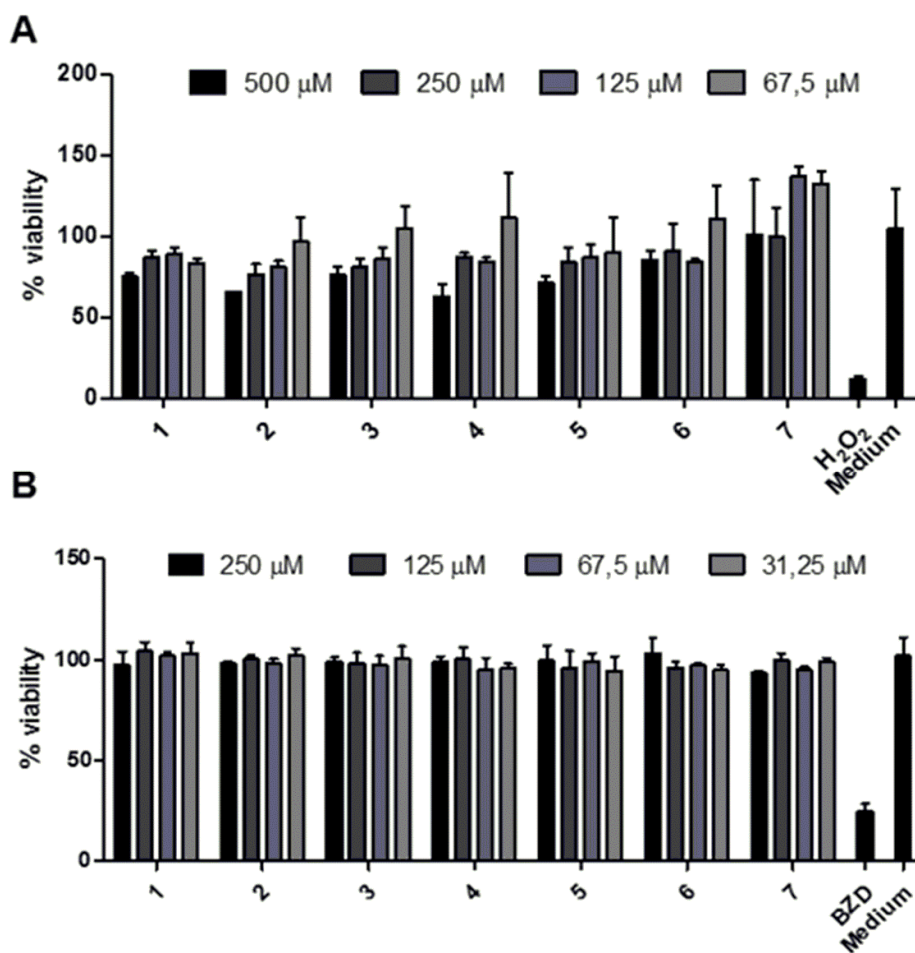


Figure 4. Evaluation of cytotoxicity and trypanocidal effect of compounds **1-7**. (A) Cytotoxicity of compounds **1-7** in LLCMK2 fibroblasts assessed by MTT; (B) Trypanocidal effect of compounds **1-7** by rezasurin method, both after 48-hours treatment. BZD, benznidazole as a reference trypanocidal drug.

2.2.2. Inhibition of *T. cruzi* trans-sialidase (TcTS)

The inhibitory activities of compounds **1-7** against *T. cruzi* trans-sialidase were evaluated by the continuous fluorimetric method, which is based on TcTS-catalyzed hydrolysis of 2'-(4-methylumbelliferyl)- α -D-N-acetyl-neuraminic acid (MuNANA), with release of the methylumbelliferone (MU) fluorophore.³⁷ Compounds **1-7** were tested at 1.0 mM concentration in the presence of MuNANA (0.1 mM), and in parallel to the measured activities of pyridoxal phosphate (PLP), used as positive control at the same concentration.³⁸

According to the Fig. 5, highest inhibition of TcTS was verified for compound **2** (88%), the N-acetamide derivative, whereas almost no inhibitory activity was detected for the other compounds (4.5-16%). Since these results did not correlate with the low parasite infection index values verified for compounds **3** and **5**, we may say that TcTS inhibition was not a possible mechanism by which these compounds blocked *T. cruzi* cell invasion.

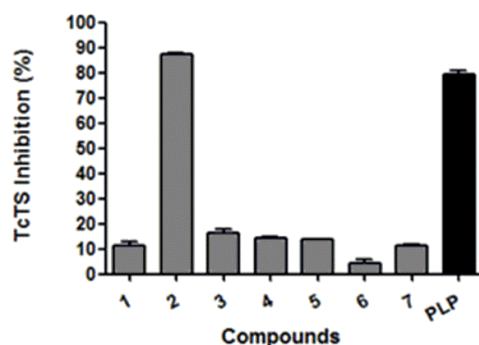


Figure 5. TcTS inhibition by compounds **1-7** performed by fluorimetric assay; PLP-pyridoxal phosphate, used as positive control.

2.2.3. Galectin-3 binding assays

Compounds **1-7** were applied to human recombinant galectin-3 (hr galectin-3)³⁹ binding assays using the Corning Epic label-free technology, which measures changes in the refraction index upon a binding event.⁴⁰ Given the partial insolubility of compounds **1-7**, they were firstly dissolved in pure DMSO and then diluted to the final working concentrations with a 1% or 2%

residual solvent. Compounds **1-7** tested in the presence of only 1% DMSO did not provide binding curves of sufficient quality for the determination of binding values, which led us to test them in the presence of 2% DMSO. In this case, signals obtained with compounds **1** through **5** were stronger and showed the expected dose-response trend (Fig. 6). By fitting of data with a non-linear algorithm, we determined the EC₅₀ binding values for compounds **1-5** (Table 1), which ranged from 17 μ M, for the highest affinities for compounds **3** and **5**, up to 200 μ M for the remaining compounds. Regarding compounds **6** and **7**, upon fitting, the obtained data did not converge to a meaningful value.

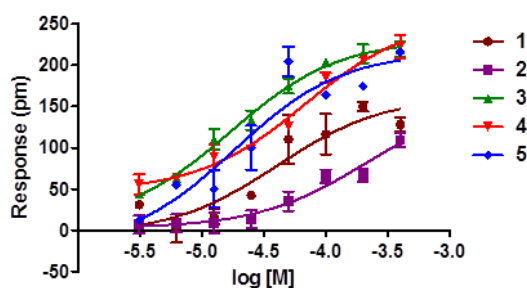


Figure 6. Dose-response binding curves of compounds **1-5** to hr galectin-3. Compounds **1-5** dissolved in PBS 1X, DMSO 2% at pH 7.4 were tested at concentrations ranging between 3 μ M and 400 μ M, on μ -plate surfaces coated with galectin-3. Results were analyzed using the EnSpire label-free user interface software. Graphs were generated using GraphPad Prism V-5.01 (GraphPad Software, La Jolla, CA). Results are means of triplicates.

Table 1. EC₅₀ values of compounds **1-5** towards hr galectin-3.

Compound	EC ₅₀ (μ M)
1	40.7
2	205
3	17.2
4	67.7
5	18.3

The higher binding affinities to galectin-3 observed for compounds **3** (17.2 μ M) and **5** (18.3 μ M) were in agreement with their increased capacities to block *T. cruzi* cell invasion. Thus, we

believe that galectin-3 inhibition by compounds **3** and **5** may have blocked the host cell infection process, contributing to its destruction still in the vacuole, considering the essential role of galectin-3 in the escape of *T. cruzi* from the parasitophorous vacuole to the cell cytoplasm, which is an important phenomenon for the permanence and multiplication of the parasite.¹⁹ To corroborate this hypothesis, we performed a Western Blotting (WB) assay to investigate the galectin-3 expression by LLCMK2 fibroblasts. In fact, galectin-3 was detected in LLCMK2 cell extracts, being verified a band with the same molecular weight of hr galectin-3 (data not shown).

2.2.3.1. Molecular modeling studies with hr galectin-3

As label-free assays showed effective binding to hr galectin-3 for most tested compounds, we found valuable to assess their theoretical binding to hr galectin-3 by molecular modeling studies.

Hence, relative affinities of compounds **1-7** towards hr galectin-3 were estimated by the MM/PBSA method in combination with molecular dynamics simulations,^{41,42} which showed compounds **3** and **5** as the ones with higher affinities for hr galectin-3 followed by compounds **1**, **2**, **4**, **6** and **7** (Table 2). These data agreed with experimental results for the EC₅₀ measured with the immobilized protein. Actually, for the condition with 1% DMSO, the compounds that showed relative affinities higher than -5 kcal/mol did not converge in the experiments, as a consequence of their low affinities towards the protein. On the other hand, the linear correlation between the data obtained with 2% DMSO and the MM/PBSA method was R²=0.31 for all compounds with converged EC₅₀ values and R²=0.96, if we consider compound **2** as an outlier (Fig. S15).

Table 2. Relative affinities of compounds **1-7** to hr galectin-3 as calculated using the MM/PBSA method.

Compound	Relative affinity [kcal/mol]
1	-6.5 ± 0.8
2	-5 ± 1
3	-9.7 ± 0.9
4	-3.3 ± 0.8
5	-11.1 ± 0.9
6	0 ± 1
7	0 ± 1

From the structural point of view, the galactose portion of compounds **1-7** kept the same interactions at the conserved carbohydrate binding site of hr galectin-3 that LacNAc displays in the crystallographic structure.²⁹ The main interactions between compounds **1-7** and residues outside the carbohydrate binding site are stacking with residues Pro-117 and Arg-144 and hydrogen bonding with Ser-237 (Fig. 7). However, residue-wise decomposition of the MM/PBSA energies showed that Pro-117 is the only residue outside the carbohydrate binding site that contributes favorably to the interaction. The interactions with Arg-144 and Ser-237 are unfavorable to the binding because of the high energetic cost associated with breaking their interaction with water from the solvent.

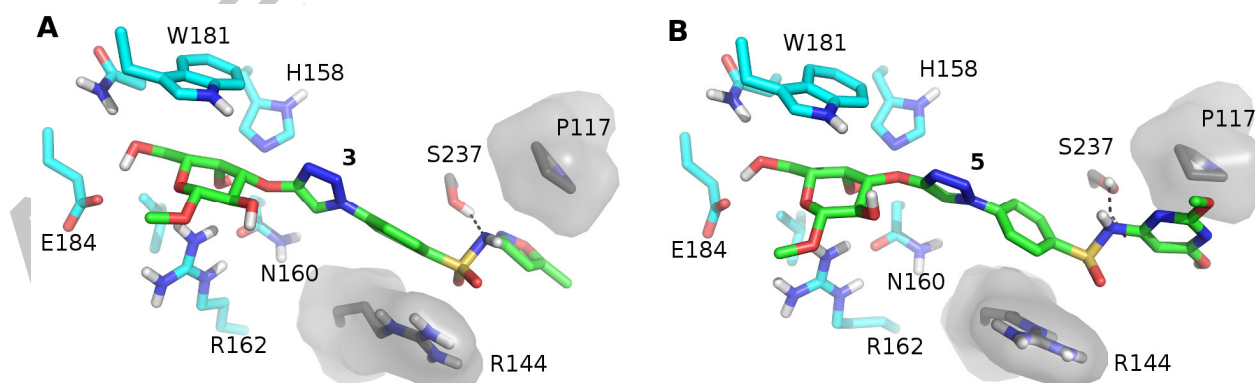


Figure 7. Representative snapshots from the molecular dynamics trajectories showing the main interactions between hr galectin-3 and representative compounds **3** (A) and **5** (B). All hydrogen, nitrogen, oxygen and sulfur atoms are displayed in white, blue, red and yellow, respectively.

Carbon atoms of the ligand are displayed in green and from residues of the carbohydrate binding site are displayed in cyan. Pro-117, Arg-144 and Ser-237 are displayed with gray carbons. Additionally, stacking interactions are highlighted by surface representation of the ligand, Pro-117 and Arg-144.

3. Conclusions

In summary, we have synthesized the O-3 triazole-linked galactosyl arylsulfonamides **1-7** from different azide arylsulfonamides and alkyne-functionalized galactose as precursors. In this regard, the use of Cu(I)-catalyzed azide-alkyne cycloaddition reaction proved to be effective for generating modified O-3 1,2,3-triazole derivatives of galactose as potential anti-trypanosomal agents.

The inhibition assays of *T. cruzi* cell invasion showed compounds **3** and **5** as the most potent in blocking parasite invasion, with reduced values of infection index (~20). Subsequently, fluorimetric inhibitory assays of compounds **1-7** against *T. cruzi* trans-sialidase (TcTS) showed highest TcTS inhibition for compound **2** (88%), whilst evaluation of their binding to hr galectin-3 using the Corning Epic label-free technology displayed higher binding affinities for compounds **3** (EC₅₀ 17.2 μM) and **5** (EC₅₀ 18.3 μM). In agreement with these later experimental results, the assessment of the theoretical binding of compounds **1-7** to hr galectin-3 by MM/PBSA method also showed higher affinities for compounds **3** (-9.7 Kcal/ mol) and **5** (-11.1 Kcal/ mol), which, in addition, established effective interactions with galectin-3 active site. Overall, compounds **3** and **5** that showed higher capacity of inhibiting fibroblast cells invasion by *T. cruzi* are the ones with higher experimental and theoretical binding affinities for hr galectin-3. Thus, these results highlight compounds **3** and **5** as potential *T. cruzi* cell invasion blockers by means of a galectin-3 binding-related mechanism, revealing galectin-3 as an important host target for design of novel anti-trypanosomal agents.

4. Experimental

4.1. General

All chemicals were purchased as reagent grade and used without further purification. Reactions were monitored by thin layer chromatography (TLC) on 0.25 mm precoated silica gel plates (Whatman, AL SIL G/UV, aluminium backing) with the indicated eluents. Compounds were visualized under UV light (254 nm) and/or dipping in ethanol-sulfuric acid (95:5, v/v), followed by heating the plate for a few minutes. Column chromatography was performed on silica gel 60 (Fluorochem, 35-70 mesh). Nuclear magnetic resonance spectra were recorded on Bruker Advance DRX 300 (300 MHz), DPX 400 (400 MHz) or DPX 500 (500 MHz) spectrometers. Chemical shifts (δ) are given in parts per million downfield from tetramethylsilane. Assignments were made with the aid of HMQC and COSY experiments. Accurate mass electrospray ionization mass spectra (ESI-HRMS) were obtained using positive or negative ionization modes on a Bruker Daltonics MicroTOF II ESI-TOF mass spectrometer.

4.2. Synthesis

4.2.1. Synthesis of azide-benzenesulfonamides 8-14

Each 4-aminobenzenesulfonamide (3.0 mmol) was added in a solution of concentrated sulfuric acid (0.5 mL) and H₂O (3.0 mL) and then cooled to 0°C in an ice bath. A solution of NaNO₂ (3.0 mmol) in water (2.1 mL) was added dropwise to the reaction and left stirring for 10 minutes. After a color change to a yellowish tone and appearance of foam in the medium, solid urea (150 mg) was added followed by NaN₃ solution (9.0 mmol, 1.5 eq) in H₂O (3.2 mL) dropwise. Finally, after stirring for few minutes each reaction was filtered through Buchner funnel and washed subsequently with 5% NaHCO₃ and H₂O. Each obtained product was dried under reduced pressure and analysed by TLC, being verified at increased retention factors (R_f) if compared to the corresponding starting materials. Compounds **8-14** were obtained in corresponding yields of 38%

(**8**), 45% (**9**), 91% (**10**), 52% (**11**), 42,5% (**12**), 40% (**13**) and 76% (**14**). ^1H NMR and IR [2100 cm^{-1} (N_3)] (2100 cm^{-1}) analysis of **8-14** were in accordance with the literature.²⁸

4.2.2. Synthesis of 1,2,3-triazole-linked galactosyl arylsulfonamides 1-7

4.2.2.1. General procedure for CuAAC reactions^{29,30}

A solution of methyl-2,4,6-tri-O-acetyl-3-prop-2-ynyl- β -D-galactopyranose **15** (1 equiv), 4-azidobenzenesulfonamides **8-14** (1 equiv), sodium ascorbate (0.5 equiv) and CuSO_4 (0.1 equiv) in DMF (0.5 mL) was placed into a microwave tube. Then, the tube was sealed and submitted to microwave irradiation for 30 min (100 $^\circ\text{C}$, 150 W). The reaction was followed by TLC (EtOAc) and after completion the reaction mixture was concentrated under reduced pressure and purified by column chromatography (EtOAc/Hexane 7:3 v/v) to afford the desired 1,2,3-triazole-linked galactosyl arylsulfonamides **23-29**.

4.2.2.2. Methyl 2,4,6-tri-O-acetyl-3-O-methyl[(4-benzenesulfonamide)-1H-1,2,3-triazol-4-yl]- β -D-galactopyranoside **23**

Following procedure described in Section 4.2.2.1 the reaction of 4-azidobenzenesulfonamide **8** (30.0 mg, 0.15 mmol), methyl-2,4,6-tri-O-acetyl-3-prop-2-ynyl- β -D-galactopyranose **15** (50.0 mg, 0.15 mmol), sodium ascorbate (12.0 mg, 0.075 mmol) and CuSO_4 (0.015 mmol, 0.1 equiv) in DMF (1.0 mL) gave the product **23** as a pale yellow oil (57.8 mg, 0.10 mmol, 69%) after purification by column chromatography (EtOAc/Hexane 7:3 v/v). ^1H NMR (300 MHz, CDCl_3): δ 8.06 (s, 1H, CH-triazole), 7.99 (d, 2H, J_{ortho} 8.4 Hz, Ar-H), 7.81 (d, 2H, J_{ortho} 8.4 Hz, Ar-H), 5.72 (s, 2H, NH_2), 5.52 (d, 1H, J 2.7 Hz, H-4), 5.13 (dd, 1H, $J_{1,2}$ 7.8 Hz, $J_{2,3}$ 9.7 Hz, H-2), 4.92 (d, 1H, J_{gem} 11.9 Hz, O- CH_2 triazole), 4.78 (d, 1H, J_{gem} 11.9 Hz, O- CH_2 triazole), 4.45 (d, 1H, $J_{1,2}$ 7.8 Hz, H-1), 4.26 (d, 2H, $J_{5,6}$ 6.8 Hz, H-6, H-6'), 3.98 (t, 1H, $J_{5,6}$ 6.8 Hz, H-5), 3.88 (dd, 1H, $J_{3,4}$ 3.1 Hz, $J_{2,3}$ 9.7 Hz, H-3), 3.60 (s, 3H, OCH_3), 2.21-2.17 (s, 9H, 3x CH_3CO). ^{13}C NMR (75 MHz, CDCl_3): δ 170.8-169.7 (CH_3CO), 142.6 (C-triazole), 139.5 (Ar, C- SO_2 and C-N-triazole), 128.3 (Ar, *o*- CSO_2), 121.3 (CH-triazole),

120.4 (Ar, m-CSO₂), 102.0 (C-1), 77.9 (C-3), 70.8 (C-2), 70.6 (C-5), 66.6 (C-4), 63.6 (OCH₂), 61.9 (C-6), 56.8 (OCH₃), 21.0-20.7 (CH₃CO). ESI-HRMS: calcd. for C₁₆H₂₂N₄O₈S [M +H]⁺: 557.1548, found: 557.1537.

4.2.2.3. Methyl 2,4,6-tri-O-acetyl-3-O-methyl-N-[(phenyl)sulfonyl]acetamide-1H-1,2,3-triazol-4-yl)-β-D-galactopyranoside 24

Following procedure described in Section 4.2.2.1, the reaction of *N*-[(4-azidophenyl)sulphonyl]acetamide **9** (33.5 mg, 0.14 mmol), methyl-2,4,6-tri-O-acetyl-3-prop-2-ynyl-β-D-galactopyranose **15** (50 mg, 0.14 mmol), sodium ascorbate (13.8 mg, 0.07 mmol) and CuSO₄ (0.014 mmol, 0.1 equiv) in DMF (1.0 mL) gave the product **24** as a pale yellow oil (54.0 mg, 0.09 mmol, 64%) after purification by column chromatography (EtOAc/Hexane 1:1 v/v). ¹H NMR (300 MHz, CDCl₃): δ 7.44 (d, 2H, *J*_{ortho} 8.5 Hz, Ar-H), 7.34 (s, 1H, CH-triazole), 7.17 (d, 2H, *J*_{ortho} 8.5 Hz, Ar-H), 4.77 (d, 1H, *J* 2.7 Hz, H-4), 4.41 (dd, 1H, *J*_{1,2} 7.8 Hz, *J*_{2,3} 9.6 Hz, H-2), 4.18 (d, 1H, *J*_{gem} 12.3 Hz, O-CH₂ triazole), 4.07 (d, 1H, *J*_{gem} 12.3 Hz, O-CH₂ triazole), 3.70 (d, 1H, *J*_{1,2} 7.8 Hz, H-1), 3.54-3.51 (m, 2H, H-6, H-6'), 3.22 (t, 1H, *J*_{5,6} 6.5 Hz, H-5), 3.12 (dd, 1H, *J*_{3,4} 3.3 Hz, *J*_{2,3} 9.7 Hz, H-3), 2.87 (s, 3H, OCH₃), 1.57 (s, 3H, CH₃CO-sulfonamide), 1.49-1.47 (s, 9H, 3x CH₃CO). ¹³C NMR (75 MHz, CDCl₃): δ 170.6-169.7 (CH₃CO, CO-sulfonamide), 146.2 (C-triazole), 142.3 (Ar, C-SO₂), 139.7 (Ar, C-N-triazole), 128.4 (Ar, *o*-CSO₂), 121.0 (CH-triazole), 120.5 (Ar, m-CSO₂), 101.9 (C-1), 78.0 (C-3), 70.8 (C-2), 70.6 (C-5), 66.6 (C-4), 63.8 (OCH₂), 61.8 (C-6), 56.8 (OCH₃), 20.9-20.7 (CH₃CO, CH₃-sulfonamide). ESI-HRMS: calcd. for C₁₈H₂₄N₄O₉S [M+H]⁺: 599.1654, found: 599.1677.

4.2.2.4. Methyl 2,4,6-tri-O-acetyl-3-O-methyl-N-[(5-methylisoxazol-3-yl)benzenesulfonamide]-1H-1,2,3-triazol-4-yl)-β-D-galactopyranoside 25

Following procedure described in Section 4.2.2.1, the reaction of 4-azido-*N*-(5-methylisoxazol-3-yl) benzenesulfonamide **10** (25.2 mg, 0.09 mmol), methyl-2,4,6-tri-O-acetyl-3-

prop-2-ynyl- β -D-galactopyranose **15** (34.0 mg, 0.09 mmol), sodium ascorbate (9.0 mg, 0.045 mmol) and CuSO₄ (0.009 mmol, 0.1 equiv) in DMF (0.8 mL) gave the product **25** as a pale yellow oil (38.1 mg, 0.06 mmol, 66%) after purification by column chromatography (EtOAc/Hexane 6:4 v/v). ¹H NMR (300 MHz, CDCl₃): δ 8.03 (s, 1H, CH-triazole), 7.99 (d, 2H, J_{ortho} 8.4 Hz, Ar-H), 7.85 (d, 2H, J_{ortho} 8.4 Hz, Ar-H), 6.25 (s, 1H, H-isoxazole), 5.48 (d, 1H, J 3.2 Hz, H-4), 5.15 (dd, 1H, $J_{1,2}$ 7.8 Hz, $J_{2,3}$ 9.6 Hz, H-2), 4.91 (d, 1H, J_{gem} 12.3 Hz, O-CH₂ triazole), 4.79 (d, 1H, J_{gem} 12.3 Hz, O-CH₂ triazole), 4.43 (d, 1H, $J_{1,2}$ 7.8 Hz, H-1), 4.24-4.27 (m, 2H, H-6, H-6'), 3.95 (t, 1H, $J_{5,6}$ 6.5 Hz, H-5), 3.85 (dd, 1H, $J_{3,4}$ 3.3 Hz, $J_{2,3}$ 9.8 Hz, H-3), 3.60 (s, 3H, OCH₃), 2.52 (s, 3H, CH₃-isoxazole), 2.29-2.17 (s, 9H, 3x CH₃CO). ¹³C NMR (75 MHz, CDCl₃): δ 171.3 (C-O-isoxazole), 170.6-169.7 (CH₃CO), 157.3 (C-N-isoxazole), 146.2 (C-triazole), 142.3 (Ar, C-SO₂), 139.1 (Ar, C-N-triazole), 129.1 (Ar, *o*-CSO₂), 121.1 (CH-triazole), 120.5 (Ar, *m*-CSO₂), 101.9 (C-1), 95.6 (CH-isoxazole), 77.9 (C-3), 70.8 (C-2), 70.6 (C-5), 66.7 (C-4), 63.7 (OCH₂), 61.8 (C-6), 56.8 (OCH₃), 21.0-20.6 (CH₃CO), 12.7 (CH₃-isoxazole). ESI-HRMS: calcd. for C₂₀H₂₅N₅O₉S [M + H]⁺: 638.1763, found: 638.1785.

4.2.2.5. Methyl 2,4,6-tri-O-acetyl-3-O-methyl-*N*-{[(4,6-dimethylpyrimidin-2-yl) benzenesulfonamide]-1*H*-1,2,3-triazol-4-yl}- β -D-galactopyranoside **26**

Following procedure described in Section 4.2.2.1, the reaction of 4-azido-*N*-(4,6-dimethylpyrimidin-2-yl) benzenesulfonamide **11** (34.0 mg, 0.11 mmol), methyl-2,4,6-tri-O-acetyl-3-prop-2-ynyl- β -D-galactopyranose **15** (40.0 mg, 0.11 mmol), sodium ascorbate (11.0 mg, 0.055 mmol) and CuSO₄ (0.011 mmol, 0.1 equiv) in DMF (1.0 mL) gave the product **26** as a pale yellow oil (42.2 mg, 0.064 mmol, 58%) after purification by column chromatography (EtOAc/Hexane 6:4 v/v). ¹H NMR (300 MHz, CDCl₃): δ 8.29 (d, 2H, J_{ortho} 8.6 Hz, Ar-H), 8.02 (s, 1H, CH-triazole), 7.87 (d, 2H, J_{ortho} 8.6 Hz, Ar-H), 6.67 (s, 1H, H-pyrimidine), 5.49 (d, 1H, J 2.6 Hz, H-4), 5.15 (dd, 1H, $J_{1,2}$ 7.8 Hz, $J_{2,3}$ 9.6 Hz, H-2), 4.92 (d, 1H, J_{gem} 12.2 Hz, O-CH₂ triazole), 4.79 (d, 1H, J_{gem} 12.2 Hz, O-CH₂ triazole), 4.43 (d, 1H, $J_{1,2}$ 7.8 Hz, H-1), 4.28-4.25 (m, 2H, H-6, H-6'), 3.95 (t, 1H, $J_{5,6}$

6.3 Hz, H-5), 3.84 (dd, 1H, $J_{3,4}$ 3.3 Hz, $J_{2,3}$ 9.6 Hz, H-3), 3.60 (s, 3H, OCH₃), 2.53 (s, 6H, 2x CH₃-pyrimidine), 2.30-2.17 (s, 9H, 3x CH₃CO). ¹³C NMR (75 MHz, CDCl₃): δ 170.5-169.6 (CH₃CO), 168.3 (C-2'), 155.9 (C-4' and C-6'), 146.1 (C-triazole), 140.0 (Ar, C-SO₂), 139.9 (Ar, C-N-triazole), 130.8 (Ar, *o*-CSO₂), 121.0 (CH-triazole), 119.7 (Ar, *m*-CSO₂), 115.1 (C-5'), 102.0 (C-1), 77.8 (C-3), 70.8 (C-2), 70.5 (C-5), 66.6 (C-4), 63.8 (OCH₂), 61.7 (C-6), 56.8 (OCH₃), 23.5 (CH₃-pyrimidine), 20.9-20.6 (CH₃CO). ESI-HRMS: calcd. for C₂₈H₃₄N₆O₁₁S [M + H]⁺: 663.2079, found: 663.2066.

4.2.2.6. Methyl 2,4,6-tri-O-acetyl-3-O-methyl-N-[[4,6-dimethoxypyrimidin-4-yl] benzenesulfonamide] -1H-1,2,3-triazol-4-yl]-β-D-galactopyranoside **27**

Following procedure described in Section 4.2.2.1, the reaction of 4-azido-*N*-(2,6-dimethoxypyrimidin-4-yl) benzenesulfonamide **12** (36.0 mg, 0.11 mmol), methyl-2,4,6-tri-O-acetyl-3-prop-2-ynyl-β-D-galactopyranose **15** (38.0 mg, 0.11 mmol), sodium ascorbate (11.0 mg, 0.055 mmol) and CuSO₄ (0.011 mmol, 0.1 equiv) in DMF (1.0 mL) gave the product **26** as a pale yellow oil (36 mg, 0.051 mmol, 47%) after purification by column chromatography (EtOAc/Hexane 7:3 v/v). ¹H NMR (300 MHz, CDCl₃): δ 8.10 (d, 2H, J_{ortho} 7.7 Hz, Ar-H), 8.04 (s, 1H, CH-triazole), 7.89 (d, 2H, J_{ortho} 7.8 Hz, Ar-H), 6.23 (s, 1H, H-pyrimidine), 5.48 (d, 1H, J 2.8 Hz, H-4), 5.14 (dd, 1H, $J_{1,2}$ 7.8 Hz, $J_{2,3}$ 9.6 Hz, H-2), 4.91 (d, 1H, J_{gem} 12.0 Hz, O-CH₂ triazole), 4.79 (d, 1H, J_{gem} 12.1 Hz, O-CH₂ triazole), 4.43 (d, 1H, $J_{1,2}$ 7.8 Hz, H-1), 4.27-4.24 (m, 2H, H-6, H-6'), 3.94 (t, 1H, $J_{5,6}$ 6.4 Hz, H-5), 3.84 (dd, 1H, $J_{3,4}$ 3.1 Hz, $J_{2,3}$ 9.7 Hz, H-3), 3.60 (s, 3H, OCH₃), 3.58 (s, 6H, 2x OCH₃-pyrimidine), 2.29-2.17 (s, 9H, 3x CH₃CO). ¹³C NMR (75 MHz, CDCl₃): δ 172.7 (C-6'), 170.6-169.7 (CH₃CO), 164.4 (C-2'), 158.6 (C-4'), 146.2 (C-triazole), 140.2 (Ar, C-SO₂), 139.5 (Ar, C-N-triazole), 129.4 (Ar, *o*-CSO₂), 121.0 (CH-triazole), 120.5 (Ar, *m*-CSO₂), 101.9 (C-1), 85.9 (C-5'), 77.9 (C-3), 70.8 (C-2), 70.6 (C-5), 66.6 (C-4), 63.8 (OCH₂), 61.7 (C-6), 56.8 (OCH₃), 54.9 (OCH₃-methoxazole), 54.3 (OCH₃-methoxazole), 20.9-20.6 (CH₃CO). ESI-HRMS: calcd. for C₂₈H₃₄N₆O₁₃S [M + H]⁺: 695.1977, found: 695.1980.

4.2.2.7. Methyl 2,4,6-tri-O-acetyl-3-O-methyl-N-[(benzenesulfa-ortho-pyridine)-1H-1,2,3-triazol-4-yl]- β -D-galactopyranoside **28**

Following procedure described in Section 4.2.2.1, the reaction of 4-azido-N-pyridin-2-yl benzenesulfonamide **13** (40.0 mg, 0.16 mmol), methyl-2,4,6-tri-O-acetyl-3-prop-2-ynyl- β -D-galactopyranose **15** (50.0 mg, 0.16 mmol), sodium ascorbate (16.0 mg, 0.08 mmol) and CuSO₄ (0.016 mmol, 0.1 equiv) in DMF (1.0 mL) gave the product **28** as a pale yellow oil (63 mg, 0.10 mmol, 62%) after purification by column chromatography (EtOAc/Hexane 7:3 v/v). ¹H NMR (300 MHz, CDCl₃): δ 8.28 (broad s, 1H, H-pyrimidine), 8.04 (d, 2H, J_{ortho} 7.6 Hz, Ar-H), 8.00 (s, 1H, CH-triazole), 7.82 (d, 2H, J_{ortho} 7.6 Hz, Ar-H), 7.70 (m, 1H, H-pyrimidine), 7.41 (broad s, 1H, H-pyrimidine), 6.83 (broad s, 1H, H-pyrimidine), 5.46 (d, 1H, $J_{3,4}$ 3.0 Hz, H-4), 5.10 (t, 1H, $J_{1,2} = J_{2,3}$ 8.54 Hz, H-2), 4.87 (d, 1H, J_{gem} 12.2 Hz, O-CH₂ triazole), 4.76 (d, 1H, J_{gem} 12.2 Hz, O-CH₂ triazole), 4.40 (d, 1H, $J_{1,2}$ 7.7 Hz, H-1), 4.22 (d, 2H, $J_{5,6}$ 6.4 Hz, H-6, H-6'), 3.92 (t, 1H, $J_{5,6}$ 6.3 Hz, H-5), 3.82 (dd, 1H, $J_{3,4}$ 3.0 Hz, $J_{2,3}$ 9.7 Hz, H-3), 3.57 (s, 3H, OCH₃), 2.26-2.13 (s, 9H, 3x CH₃CO). ¹³C NMR (75 MHz, CDCl₃): δ 170.4-169.5(CH₃CO), 155.5 (C-2'), 146.0 (C-triazole), 143.1 (C-6'), 139.5 (Ar, C-SO₂), 139.2 (C-3'), 139.5 (Ar, C-N-triazole), 128.6 (Ar, *o*-CSO₂), 121.1 (C-H triazole), 120.5 (Ar, *m*-CSO₂), 115.8 (C-4'), 113.9 (C-5'), 101.9 (C-1), 70.8 (C-2), 70.5 (C-5), 66.6 (C-4), 63.7 (OCH₂), 61.7 (C-6), 56.8 (OCH₃), 20.8-20.6 (CH₃CO). ESI-HRMS: calcd. for C₂₇H₃₁N₅O₁₁S [M + H]⁺: 634.1814, found: 634.1836.

4.2.2.8. Methyl 2,4,6-tri-O-acetyl-3-O-methyl-N-[(4-methylpyrimidin-2-yl)benzenesulfonamide]-1H-1,2,3-triazol-4-yl]- β -D-galactopyranoside **29**

Following procedure described in Section 4.2.2.1, the reaction of 4-azido-N-(4-methylpyrimidin-2-yl) benzenesulfonamide **14** (26.2 mg, 0.09 mmol), methyl-2,4,6-tri-O-acetyl-3-prop-2-ynyl- β -D-galactopyranose **15** (34.0 mg, 0.09 mmol), sodium ascorbate (9.0 mg, 0.045 mmol) and CuSO₄ (0.009 mmol, 0.1 equiv) in DMF (0.8 mL) gave the product **29** as a pale yellow oil (57.8 mg, 0.10 mmol, 69%) after purification by column chromatography (EtOAc/Hexane 7:3

v/v). ^1H NMR (300 MHz, CDCl_3): δ 8.42 (broad s, 1H, H-pyrimidine), 8.29 (d, 2H, J_{ortho} 8.3 Hz, Ar-H), 8.01 (s, 1H, CH-triazole), 7.88 (d, 2H, J_{ortho} 8.6 Hz, Ar-H), 6.83 (m, 1H, H-pyrimidine), 5.48 (d, 1H, $J_{3,4}$ 2.9 Hz, H-4), 5.48 (dd, 1H, $J_{1,2}$ 7.9 Hz, $J_{2,3}$ 9.5 Hz, H-2), 5.15 (d, 1H, J_{gem} 11.9 Hz, O- CH_2 triazole), 4.92 (d, 1H, J_{gem} 11.9 Hz, O- CH_2 triazole), 4.43 (d, 1H, $J_{1,2}$ 7.8 Hz, H-1), 4.28-4.25 (m, 2H, H-6, H-6'), 3.96 (t, 1H, $J_{5,6}$ 6.3 Hz, H-5), 3.84 (dd, 1H, $J_{3,4}$ 2.9 Hz, $J_{2,3}$ 9.7 Hz, H-3), 3.61 (s, 3H, OCH_3), 2.58 (s, 3H, CH_3 -pyrimidine), 2.53 (s, 6H, 2x CH_3 -pyrimidine), 2.30-2.17 (s, 9H, 3x CH_3CO). ^{13}C NMR (75 MHz, CDCl_3): δ 170.5-170.4 (CH_3CO), 169.6 (C-2'), 156.8 (C-4'), 146.1 (C-triazole), 140.0 (Ar, C- SO_2), 139.9 (Ar, C-N-triazole), 130.8 (Ar, *o*- CSO_2), 121.0 (CH-triazole), 119.8 (Ar, *m*- CSO_2), 115.2 (C-5'), 102.0 (C-1), 77.9 (C-3), 70.8 (C-2), 70.6 (C-5), 66.6 (C-4), 63.8 (OCH_2), 61.7 (C-6), 56.8 (OCH_3), 24.1 (CH_3 -pyrimidine), 20.9-20.6 (CH_3CO). ESI-HRMS: calcd. for $\text{C}_{27}\text{H}_{32}\text{N}_6\text{O}_{11}\text{S}$ [$\text{M} + \text{H}$] $^+$: 649.1923, found: 649.1930.

4.2.3. General procedure for deacetylation reactions²⁹

To the solutions of compounds **23-29** in methanol (2.0 mL) was added 1 M NaOMe until pH 9–10 was achieved. The mixtures were stirred for 2-4 h at room temperature, neutralized with ion exchange resin (Dowex 50WX8-200 H+), filtered and concentrated under reduced pressure.

4.2.3.1. Methyl-3-O-methyl[(4-benzenesulfonamide)-1H-1,2,3-triazol-4-yl]- β -D-galactopyranoside **1**

Following the procedure described in Section 4.2.3. deacetylation reaction of compound **24** (55 mg, 0.01 mmol) under conditions described gave the final product **1** as a white amorphous solid (29.9 mg, 0.007 mmol, 70.2%). ^1H NMR (400 MHz, D_2O): δ 8.41 (s, 1H, CH-triazole), 7.92 (d, 2H, J_{ortho} 8.8 Hz, Ar-H), 7.86 (d, 2H, J_{ortho} 8.8 Hz, Ar-H), 5.02 (dd, 1H, $J_{1,2}$ 7.8 Hz, $J_{2,3}$ 9.7 Hz, H-2), 4.79 (d, 1H, J_{gem} 12.2 Hz, O- CH_2 triazole), 4.64 (d, 1H, J_{gem} 12.2 Hz, O- CH_2 triazole), 4.29 (d, 1H, $J_{1,2}$ 7.8 Hz, H-1), 4.14 (d, 1H, $J_{3,4}$ 3.4 Hz, H-4), 3.77-3.73 (m, 2H, H-6, H-6'), 3.66 (dd, 1H, $J_{3,4}$ 3.4 Hz, $J_{2,3}$ 9.7 Hz, H-3), 3.55 (t, 1H, $J_{5,6}$ 5.6 Hz, H-5), 3.42 (s, 3H, OCH_3). ^{13}C NMR (75 MHz, D_2O):

δ 146.0 (C-triazole), 143.9 (Ar, C-SO₂), 139.2 (Ar, C-N-triazole), 127.7 (Ar, *m*-CSO₂), 121.9 (CH-triazole), 120.2 (Ar, *m*-CSO₂), 102.1 (C-1), 79.5 (C-3), 75.2 (C-5), 70.9 (C-2), 65.6 (C-4), 62.0 (OCH₂), 60.9 (C-6), 55.5 (OCH₃). ESI-HRMS: calcd. for C₁₈H₂₃N₄O₉S [M - H]⁻: 471.1191, found: 471.1181.

4.2.3.2. Methyl 3-O-methyl-*N*-{[(phenyl)sulfonyl]acetamide}-1*H*-1,2,3-triazol-4-yl}- β -D-galactopyranoside **2**

Following the procedure described in Section 4.2.3. deacetylation reaction of compound **25** (18 mg, 0.03 mmol) under conditions described gave the final product **2** (13.8 mg, 0.029 mmol, 97%) as an amorphous solid. ¹H NMR (400 MHz, D₂O): δ 8.50 (s, 1H, CH-triazole), 8.07 (d, 2H, *J*_{ortho} 8.3 Hz, Ar-H), 7.93 (d, 2H, *J*_{ortho} 8.3 Hz, Ar-H), 5.00 (dd, 1H, *J*_{1,2} 7.8 Hz, *J*_{2,3} 9.7 Hz, H-2), 4.72 (broad s, 2H, O-CH₂ triazole), 4.33 (d, 1H, *J*_{1,2} 6.7 Hz, H-1), 4.80-4.90 (m, 1H, H-2), 4.22 (d, 1H, *J*_{3,4} 2.5 Hz, H-4), 3.79 (d, 1H, *J*_{5,6} 4.0 Hz, H-5), 3.58 (broad s, 2H, H-6, H-6'), 3.51 (d, 1H, *J*_{3,4} 2.5 Hz, H-3), 3.37 (s, 3H, OCH₃), 2.14 (s, 3H, CH₃CO-sulfonamide). ¹³C NMR (75 MHz, D₂O): δ 170.5 (CO-sulfacetamide), 146.0 (C-triazole), 143.9 (Ar, C-SO₂), 139.2 (Ar, C-N-triazole), 127.7 (Ar, *m*-CSO₂), 121.9 (CH-triazole), 120.2 (Ar, *m*-CSO₂), 102.1 (C-1), 79.5 (C-3), 75.2 (C-5), 70.9 (C-2), 65.6 (C-4), 62.0 (OCH₂), 60.9 (C-6), 55.5 (OCH₃), 23.6 (CH₃-sulfacetamide). ESI-HRMS: calcd. for C₁₈H₂₄N₄O₉S [M + Na]⁺: 495.1156, found: 495.1156.

4.2.3.3. Methyl 3-O-methyl-*N*-{[(5-methylisoxazol-3-yl)benzenesulfonamide]-1*H*-1,2,3-triazol-4-yl}- β -D-galactopyranoside **3**

Following the procedure described in Section 4.2.3. deacetylation reaction of compound **25** (35 mg, 0.055 mmol) under conditions described gave the final product **3** (28 mg, 0.055 mmol, 100%) as an amorphous solid. ¹H NMR (400 MHz, D₂O): δ 8.40 (s, 1H, CH-triazole), 7.92 (d, 2H, *J*_{ortho} 8.5 Hz, Ar-H), 7.87 (d, 2H, *J*_{ortho} 8.5 Hz, Ar-H), 6.05 (s, 1H, H-isoxazole), 5.02 (dd, 1H, *J*_{1,2} 7.8 Hz, *J*_{2,3} 9.7 Hz, H-2), 4.79 (d, 1H, *J*_{gem} 12.3 Hz, O-CH₂ triazole), 4.64 (d, 1H, *J*_{gem} 12.3 Hz, O-

CH₂ triazole), 4.29 (d, 1H, $J_{1,2}$ 7.8 Hz, H-1), 4.13 (d, 1H, $J_{3,4}$ 2.8 Hz, H-4), 3.77-3.74 (m, 2H, H-6, H-6'), 3.65 (dd, 1H, $J_{3,4}$ 2.8 Hz, $J_{2,3}$ 9.7 Hz, H-3), 3.54 (t, 1H, $J_{5,6}$ 5.6 Hz, H-5), 3.42 (s, 3H, OCH₃), 2.32 (s, 1H, CH₃-isoxazole). ¹³C NMR (75 MHz, D₂O): δ 171.0 (C-O-isoxazole), 157.6 (C=N-isoxazole), 146.0 (C-triazole), 140.1 (Ar, C-SO₂), 139.6 (Ar, C-N-triazole), 128.9 (Ar, *m*-CSO₂), 122.0 (CH-triazole), 120.4 (Ar, *p*-CSO₂), 102.1 (C-1), 95.1 (CH-isoxazole), 79.5 (C-3), 75.1 (C-5), 70.9 (C-2), 65.6 (C-4), 61.9 (OCH₂), 60.9 (C-6), 55.5 (OCH₃), 10.9 (CH₃-isoxazole). ESI-HRMS: calcd. for C₂₂H₂₇N₅O₁₀S [M - H]⁻: 552.1406, found: 552.1417.

4.2.3.4. Methyl 3-O-methyl-*N*-{[(4,6-dimethylpyrimidin-2-yl) benzenesulfonamide]-1H-1,2,3-triazol-4-yl}-β-D-galactopyranoside 4

Following the procedure described in Section 4.2.3. deacetylation reaction of compound **26** (39 mg, 0.059 mmol) under conditions described gave the final product **4** (20 mg, 0.037 mmol, 63%) as an amorphous solid. ¹H NMR (400 MHz, D₂O): δ 8.39 (s, 1H, CH-triazole), 8.06 (d, 2H, J_{ortho} 8.5 Hz, Ar-H), 7.84 (d, 2H, J_{ortho} 8.5 Hz, Ar-H), 6.55 (s, 1H, H-pyrimidine), 5.00 (dd, 1H, $J_{1,2}$ 7.8 Hz, $J_{2,3}$ 9.6 Hz, H-2), 4.79 (d, 1H, J_{gem} 12.2 Hz, O-CH₂ triazole), 4.62 (d, 1H, J_{gem} 12.3 Hz, O-CH₂ triazole), 4.27 (d, 1H, $J_{1,2}$ 7.8 Hz, H-1), 4.10 (d, 1H, $J_{3,4}$ 2.9 Hz, H-4), 3.74-3.71 (m, 2H, H-6, H-6'), 3.62 (dd, 1H, $J_{3,4}$ 2.9 Hz, $J_{2,3}$ 9.6 Hz, H-3), 3.51 (t, 1H, $J_{5,6}$ 6.1 Hz, H-5), 3.40 (s, 3H, OCH₃), 2.30 (s, 6H, 2x CH₃-pyrimidine). ¹³C NMR (75 MHz, D₂O): δ 171.9 (C-2'), 157.6 (C-6', C-4'), 147.3 (C-triazole), 142.8 (Ar, C-SO₂), 140.9 (Ar, C-N-triazole), 131.4 (Ar, *m*-CSO₂), 123.4 (CH-triazole), 120.9 (Ar, *p*-CSO₂), 114.1 (C-5'), 103.5 (C-1), 80.9 (C-3), 76.6 (C-5), 72.3 (C-2), 67.0 (C-4), 63.2 (OCH₂), 62.3 (C-6), 56.9 (OCH₃), 21.0 (CH₃-pyrimidine). ESI-HRMS: calcd. for C₂₄H₃₀N₆O₉S [M + Na]⁺: 601.1687, found: 601.1708.

4.2.3.5. Methyl 3-O-methyl-*N*-{[(4,6-dimethoxypyrimidin-4-yl) benzenesulfonamide] -1H-1,2,3-triazol-4-yl}-β-D-galactopyranoside 5

Following the procedure described in Section 4.2.3. deacetylation reaction of compound **27**

(32 mg, 0.046 mmol) under conditions described gave the final product **5** (26.4 mg, 0.046 mmol, 100%) as an amorphous solid. ^1H NMR (400 MHz, D_2O): δ 8.39 (s, 1H, CH-triazole), 8.0 (d, 2H, J_{ortho} 8.5 Hz, Ar-H), 7.88 (d, 2H, J_{ortho} 8.5 Hz, Ar-H), 5.95 (s, 1H, H-pyrimidine), 5.01 (dd, 1H, $J_{1,2}$ 7.8 Hz, $J_{2,3}$ 9.6 Hz, H-2), 4.79 (d, 1H, J_{gem} 12.2 Hz, O-CH₂ triazole), 4.63 (d, 1H, J_{gem} 12.3 Hz, O-CH₂ triazole), 4.28 (d, 1H, $J_{1,2}$ 7.8 Hz, H-1), 4.11 (d, 1H, $J_{3,4}$ 3.0 Hz, H-4), 3.80 (s, 3H, OCH₃ pyrimidine), 3.79 (s, 3H, OCH₃ pyrimidine), 3.75-3.72 (m, 2H, H-6, H-6'), 3.64 (dd, 1H, $J_{3,4}$ 3.0 Hz, $J_{2,3}$ 9.6 Hz, H-3), 3.53 (t, 1H, $J_{5,6}$ 6.1 Hz, H-5), 3.41 (s, 3H, OCH₃). ^{13}C NMR (75 MHz, D_2O): δ 174.1 (C-6'), 161.2 (C-4', C-2'), 147.4 (C-triazole), 141.8 (Ar, C-SO₂), 141.4 (Ar, C-N-triazole), 130.6 (Ar, *m*-CSO₂), 123.4 (CH-triazole), 121.7 (Ar, *p*-CSO₂), 103.5 (C-1), 86.20 (C-5'), 80.9 (C-3), 76.6 (C-5), 72.3 (C-2), 67.0 (C-4), 63.3 (OCH₂), 62.4 (C-6), 56.9 (OCH₃), 55.6 (OCH₃-pyrimidine), 54.8 (OCH₃-pyrimidine). ESI-HRMS: calcd. for C₂₄H₃₀N₆O₁₁S [M + H]⁺: 611.1766, found: 611.1798.

4.2.3.6. Methyl 3-O-methyl-N-[(benzenesulfa-ortho-pyridine)-1H-1,2,3-triazol-4-yl]- β -D-galactopyranoside **6**

Following the procedure described in Section 4.2.3. deacetylation reaction of compound **28** (60 mg, 0.095 mmol) under conditions described gave the final product **6** as an amorphous solid (46.1 mg, 0.091 mmol, 95.7%). ^1H NMR (400 MHz, D_2O): δ 8.35 (s, 1H, CH-triazole), 7.91 (d, 2H, J_{ortho} 8.5 Hz, Ar-H), 7.78 (m, 3H, Ar-H, H-pyridine), 7.58 (ddd, 1H, J 1.8 Hz, J 6.7 Hz, J 8.7 Hz, H-pyridine), 7.14 (d, 1H, J 8.6 Hz, H-pyridine), 6.72 (ddd, 1H, J 0.9 Hz, J 5.7 Hz, J 6.8 Hz, H-pyridine), 4.99 (dd, 1H, $J_{1,2}$ 7.8 Hz, $J_{2,3}$ 9.7 Hz, H-2), 4.79 (d, 1H, J_{gem} 12.2 Hz, O-CH₂ triazole), 4.61 (d, 1H, J_{gem} 12.3 Hz, O-CH₂ triazole), 4.27 (d, 1H, $J_{1,2}$ 7.8 Hz, H-1), 4.11 (d, 1H, $J_{3,4}$ 3.0 Hz, H-4), 3.74-3.71 (m, 2H, H-6, H-6'), 3.63 (dd, 1H, $J_{3,4}$ 3.0 Hz, $J_{2,3}$ 9.7 Hz, H-3), 3.53 (t, 1H, $J_{5,6}$ 6.0 Hz, H-5), 3.39 (s, 3H, OCH₃). ^{13}C NMR (75 MHz, D_2O): δ 146.0 (C-triazole), 142.5 (Ar, C-SO₂), 141.9 (Ar, C-N-triazole), 139.9-139.2 (C-5' and C-2'), 128.4 (Ar, *m*-CSO₂), 121.7 (CH-triazole), 120.2 (Ar, *m*-CSO₂), 115.9-114.6 (C-3' and C-4'), 102.1 (C-1), 79.7 (C-3), 75.0 (C-5), 71.0 (C-2),

65.7 (C-4), 62.2 (OCH₂), 61.0 (C-6), 56.0 (OCH₃). ESI-HRMS: calcd. for C₂₃H₂₇N₅O₉S [M + H]⁺: 550.1602, found: 550.1621.

4.2.3.7. Methyl 3-O-methyl-N-[(4-methylpyrimidin-2-yl)benzenesulfonamide]-1H-1,2,3-triazol-4-yl]-β-D-galactopyranoside **7**

Following the procedure described in Section 3.2.3. deacetylation reaction of compound **29** (33 mg, 0.051 mmol) under conditions described gave the final product **7** as an amorphous solid (19.9 mg, 0.038 mmol, 74.7%). ¹H NMR (400 MHz, D₂O): δ 8.41 (s, 1H, CH-triazole), 8.16-8.11 (m, 3H, Ar-H, H-pyrimidine), 7.90 (d, 2H, *J*_{ortho} 8.3 Hz, Ar-H), 6.74 (s, 1H, H-pyrimidine), 5.11-5.05 (m, 1H, H-2), 4.79 (d, 1H, *J*_{gem} 12.2 Hz, O-CH₂ triazole), 4.69 (d, 1H, *J*_{gem} 12.2 Hz, O-CH₂ triazole), 4.33 (d, 1H, *J*_{1,2} 7.8 Hz, H-1), 4.16 (broad s, 1H, H-4), 3.82-3.78 (m, 2H, H-6, H-6'), 3.67 (dd, 1H, *J*_{3,4} 2.0 Hz, *J*_{2,3} 9.5 Hz, H-3), 3.55 (broad s, 1H, H-5), 3.48 (s, 3H, OCH₃), 3.34 (s, 3H, CH₃-pyrimidine). ¹³C NMR (75 MHz, D₂O): δ 169.4 (C-2'), 156.7 (C-6'), 156.5 (C-4'), 146.0 (C-triazole), 140.7 (Ar, C-SO₂), 139.7 (Ar, C-N-triazole), 130.0 (Ar, *m*-CSO₂), 121.9 (CH-triazole), 119.7 (Ar, *m*-CSO₂), 114.4 (C-5'), 102.1 (C-1), 79.6 (C-3), 75.1 (C-5), 71.0 (C-2), 65.6 (C-4), 62.0 (OCH₂), 61.0 (C-6), 55.8 (OCH₃), 22.6 (CH₃-pyrimidine). ESI-HRMS: calcd. for C₂₃H₂₈N₆O₉S [M + H]⁺: 565.1711, found: 565.1726.

4.3. Biological assays

4.3.1. Inhibition of *T. cruzi* cell invasion

Inhibition of fibroblast cells invasion by *T. cruzi* was carried out by treating with 250 μM of compounds **1-7** previously adhered LLCMK2 fibroblasts in circular coverslips (2 x 10⁴ cells per well in 500 μL of RPMI 1640 supplemented with penicillin, streptomycin, L-glutamine, and 10% FBS) and, after 30 minutes, adding 1 x 10⁵ trypomastigote forms of *T. cruzi* (in a proportion of 5 parasites for each fibroblast). The cultures were incubated for 18 hours at 37 °C and 5% CO₂, then the coverslips were fixed and stained with fast panoptic dye (Laborclin, Brazil). The coverslips

were mounted to glass slides with Entellan (Merck Millipore, USA) and examined under an optical microscope. The level of parasitic cell invasion was determined using three parameters: *i*) percentage of infected cells; *ii*) mean number of *T. cruzi* amastigotes by cell; *iii*) infection index that was determined by multiplying the percentage of infected cells times by the mean number of parasites per cell, as described previously.^{34,35}

4.3.2. Citotoxicity assay

LLCMK2 fibroblasts were seeded in 96-wells plates (1×10^4 cells in 200 μL per well) in RPMI 1640 supplemented with penicillin, streptomycin, L-glutamine, and 10% FBS. After adhering overnight at 37°C and 5% CO₂, the medium was replaced by fresh RPMI medium with different concentrations of compounds **1-7** (500 to 67,5 μM) in triplicate and cultured at 37 °C and 5% CO₂ for 48 hours. Then, 20 μL of a 5 mg/mL of (3-(4,5-Dimethylthiazol-2-yl)-2,5-Diphenyltetrazolium Bromide, MTT, Sigma-Aldrich, USA) were added to each well and incubated for 4 h at 37°C and 5% CO₂. The medium was discarded and 200 μL of dimethylsulfoxide was added to each well to dissolve formazan crystals, and then the plate was read at 570 nm (UV mini 1240, Shimadzu).

4.3.3. Trypanocidal assay

Culture derived tripomastigote forms of *T. cruzi* (Y strain) were seeded in 96-wells plates (1×10^6 cells in 200 μL per well) in RPMI 1640 supplemented with penicillin, streptomycin, L-glutamine, and 10% FBS containing different concentrations of the compounds (ranging from 250 to 31,25 μM) and incubated at 37°C and 5% CO₂ for 48 hours. Then, 5 μL of a 1 mg/mL solution of resazurin (Sigma-Aldrich, USA) were added to each well and, 6 hours after 37°C and 5% CO₂ incubation the plates were read at 570 and 600 nm (UV mini 1240, Shimadzu). The parasites viability were assessed subtracting the OD in 600 nm from the OD in 570 nm and comparing with untreated cells.

4.3.4. Inhibition of *T. cruzi* trans-sialidase (TcTS)

trans-Sialidase used in this study was a His-tagged 70 kDa recombinant material truncated to remove C-terminal repeats but retaining the catalytic N-terminal domain of the enzyme.⁴³ Inhibition was assessed using the continuous fluorimetric assay described by Douglas and co-workers.³⁷ Briefly, the assay was performed in triplicate in 96-well plates containing phosphate buffer solution at pH 7 (25 μ L), recombinant enzyme solution (25 μ L) and inhibitor solution (25 μ L of 4.0 mM solution). This mixture was incubated for 10 min. at 26 °C followed by addition of MuNANA (25 μ L of a 0.4 mM solution affording an assay concentration of 0.1 mM). The fluorescent product released was measured over 5 min., with excitation and emission wavelengths of 360 and 460 nm, respectively, and the data were analyzed with GraphPad Prism software version 4.0 (San Diego, CA, USA). Inhibition percentages were calculated according to the equation: % I = 100 \times [1 - (V_i/V_0)], where V_i is the velocity in the presence of inhibitor and V_0 is the velocity in absence of inhibitor.

4.3.5. Galectin-3 binding assays

4.3.5.1. Isolation and purification of human recombinant galectin-3

The purified preparation of hr galectin-3 was prepared as described previously³⁹ using a crude extract of transformed BL21 *E.coli* strain contained cDNA of human galectin-3 and affinity chromatography on lactosyl-Sepharose (Sigma).

4.3.5.2. Corning Epic label-free assays

Binding assays of small molecules to hr galectin-3 were performed with the Corning Epic label-free technology using the EnSpire Multimode Plate Reader.⁴⁰ Galectin-3 was immobilized on the microplate optical biosensor surface preactivated with N-hydroxy-succinimide esters groups. Protein solutions at 150 μ g/mL in 20 mM sodium acetate at pH 4.0, were dispensed into the wells (15 μ L) and left in incubation for 16 h at 4 °C. The microplate was subsequently washed three times in the binding buffer (PBS 1X, DMSO 1% or 2% at pH 7.4). A baseline reading was recorded

before and after stabilization in the binding buffer for 3 h. Given their partial insolubility in aqueous buffers, compounds were first dissolved in pure DMSO and then diluted to the final working concentrations dissolved in the binding buffer containing 1% or 2% DMSO. Compound solutions were dispensed into the wells (total volume 30 μ L) in triplicate at different concentrations, ranging from 0.09 to 400 μ M. Final readings were taken up to a period of 3 h at 25 $^{\circ}$ C. Label-free responses were measured as shifts in reflected wavelength and were expressed in picometers. The difference between the last baseline measurements and the maximum signal obtained after 3 h incubation was used to obtain plots of compound concentration versus picometers. Readings from blank wells treated with the solvent alone were further subtracted to obtain the net binding values. EC₅₀ binding values were obtained by non-linear fitting of values using a one-site ligand binding model. Results were analyzed using the EnSpire label-free user interface software. Plots were generated using GraphPad Prism V-5.01 (GraphPad Software, La Jolla, CA).

4.4. Molecular modeling studies with hr galectin-3

The 3D structure of compounds **1-7** were optimized with the RM1 semi-empirical hamiltonian⁴⁴ using the MOPAC 2016⁴⁵ software and then at the HF/6-31G* theory level using Gaussian 03. The electronic density was calculated at the same theory level for obtaining RESP charges with the antechamber package from AmberTools16.⁴⁶

The initial structure for the human galectin-3 carbohydrate recognition domain was that described by the crystallographic structure PDB ID 1KJL.⁴⁷ The initial structures of the complexes were obtained by structural alignment of the galactosyl portion of glycoconjugates **1-7** with the galactose residue from LacNAc present in the crystallographic structure.

Molecular dynamics simulations were performed with the GROMACS 5.1.2 suite⁴¹ with the AMBER99SB-ILDN forcefield⁴⁸ for describing the protein, water and ions and GAFF⁴⁹ for describing ligands. TIP3P water model was used in a dodecahedric box containing about 32 thousand atoms with about 30 NaCl to account for charge neutralization and the ionic strength of

150 mM. The system was submitted to energy minimization with the steepest descent algorithm until convergence to single precision and then to 1 ns equilibration phase using the v-rescale thermostat and berendsen barostat to keep temperature and pressure at 309K and 1bar, respectively. Production runs were carried out for 20 ns repeated 3 times from different initial velocities using the Nose-Hoover thermostat and Parrinello-Rahman barostat. The time step was 2 fs.

Estimation of the relative affinity between human galectin-3 and the ligands **1-7** was made with the MM/PBSA method as implemented in AmberTools16.⁴¹ The value for the internal dielectric constant was set to 1. A total of 100 frames of each system was used for the calculations and errors were calculated by bootstrapping with 200 resamplings. Solute entropic contributions were not calculated and, hence, the final results can only be interpreted in a comparative way to rank the compounds.

The hardware was provided by a Brazilian startup called Mining Information for You (MI4U) and was composed of machines hosted at the IBM SoftLayer infrastructure. Each of them had 24 physical cores at 2.60 GHz and two nVIDIA Tesla K80 GPUs.

Supporting Information Available: The Supporting Information encloses the ¹H NMR and ESI-MS analyses of the main compounds, as well as a complementary figure related to molecular modeling studies.

Acknowledgments

We acknowledge the financial support and fellowships from FAPESP (Fundação de Amparo à Pesquisa do Estado de São Paulo, Proc. 2012/19390-0) and CNPq (Conselho Nacional de Pesquisa e Desenvolvimento Científico e Tecnológico, Grant: 31.1947/2015-8). We are grateful to Prof. Gino Del Ponte for valuable suggestions in the synthesis of the target compounds, to Vinícius Palaretti for NMR analyses, to José Carlos Tomaz for ESI-MS analyses, to Prof. Antonio Caliri for discussions about the molecular dynamics simulations, and to Prof. Richard D. Cummings for kindly providing *E. coli* BL21 (DE3) containing the plasmid expressing human galectin-3.

References

1. Chagas Disease, fact sheet, WHO. <http://www.who.int/mediacentre/factsheets/fs340/en/>; 2017, Accessed 01.07.2017.
2. Field MC, Horn D, Fairlamb AH, Ferguson MA, Gray DW, Read KD, De Rycker M, Torrie LS, Wyatt PG, Wyllie S, Gilbert IH. Ant-trypanosomatid drug discovery: an ongoing challenge and a continuing need. *Nature Rev. Microbiol.* 2017; 15: 217-231.
3. Campo VL, Martins-Teixeira MB, Carvalho I. *Trypanosoma cruzi* invasion into host cells: A complex molecular targets interplay. *Mini Rev. Med. Chem.* 2016; 16: 1084-1097.
4. Rubin-de-Celis SSC, Schenkman S. *Trypanosoma cruzi* trans-sialidase as a multifunctional enzyme in Chagas' disease. *Cell. Microbiol.* 2012; 14: 1522-1530.
5. Buscaglia CA, Campo VA, Frasch, AC, Di Noia JM. *Trypanosoma cruzi* surface mucins: host-dependent coat diversity. *Nat. Rev. Microbiol.* 2006; 4: 229-236.
6. Gea S, Guinazu N, Pellegrini A, Carrera Silva EA, Giordanengo L, Cano R, Aoki, MP. Cruzipain, a major *Trypanosoma cruzi* cystein protease in the host-parasite interplay *Immunología.* 2006; 25: 225-238.
7. Rapoport EM, Kurmyshkina OV, Bovin, NV. Mammalian galectins: structure, carbohydrate specificity, and functions. *Biochem.(Mosc.).* 2008; 73: 393-405.
8. Cummings RD, Liu FT. In *Essentials of Glycobiology*, 2nd ed. Varki, A., Cummings, R.D., Esko, J.D., Freeze, H.H., Stanley, P., Bertozzi, C.R., Hart, G.W., Etzler, M.E., Eds.; Cold Spring Harbor Laboratory Press: New York, 2009.
9. Pellegrini A, Guinazu N, Giordanengo L, Cano RC, Gea S. The role of Toll-like receptors and adaptive immunity in the development of protective or pathological immune response triggered by the *Trypanosoma cruzi* protozoan. *Future Microbiol.* 2011;12: 1521-1533.
10. Campo VL, Aragao-Leoneti V, Martins-Teixeira MB, Carvalho I. In *New Developments in Medicinal Chemistry*. Taft, C.A.; Silva, C.H.T.d.P., Eds.; Bentham Science Publishers Ltd., 2010; 1: 133-151.
11. Buschiazzo A, Amaya MF, Cremona ML, Frasch AC, Alzari PM. The crystal structure and mode of action of trans-sialidase, a key enzyme in *Trypanosoma cruzi* pathogenesis. *Mol. Cell.* 2002; 10: 757-768.
12. Amaya MF, Watts AG, Damager I, Wehenkel A, Nguyen T, Buschiazzo A, Paris G, Frasch AC, Withers SG, Alzari PM. Structural insights into the catalytic mechanism of *Trypanosoma cruzi* trans-sialidase. *Structure.* 2004; 12: 775-784.
13. Pereira-Chioccola VL, Acosta-Serrano A, Correia de Almeida I, Ferguson MA, Souto-Padron T, Rodrigues MM, Travassos LR, Schenkman S. Mucin-like molecules form a negatively charged coat that protects *Trypanosoma cruzi* trypomastigotes from killing by human anti- α -galactosyl antibodies. *J. Cell Sci.* 2000; 113: 1299-1307.
14. Turner CW, Lima MF, Villalta F. *Trypanosoma cruzi* uses a 45-KDa mucin for adhesion to

mammalian cells. *Biochem. Biophys. Res. Commun.* 2002; 290: 29-34.

15. Rubin-de-Celis SS, Uemura H, Yoshida N, Schenkman S. Expression of trypomastigote *trans*-sialidase in metacyclic forms of *Trypanosoma cruzi* increases parasite escape from its parasitophorous vacuole. *Cell Microbiol.* 2006; 8: 1888–1898.

16. Almeida IC, Ferguson MAJ, Schenkman S, Travassos LR. GPI-anchored glycoconjugates from *Trypanosoma cruzi* trypomastigotes are recognized by lytic anti-alpha-galactosyl antibodies isolated from patients with chronic Chagas Disease. *Braz. J. Med. Biol. Res.* 1994; 27: 443-447.

17. Acosta-Serrano A, Almeida IC, Freitas-Junior LH, Yoshida N, Schenkman S. The mucin-like glycoprotein super-family of *Trypanosoma cruzi*: structure and biological roles. *Mol. Biochem. Parasitol.* 2001; 114: 143-150.

18. Moody TN, Ochieng J, Villalta F. Novel mechanism that *Trypanosoma cruzi* uses to adhere to the extracellular matrix mediated by human galectin-3. *FEBS Lett.* 2000; 470: 305-308.

19. Machado FC, Cruz L, da Silva AA, Cruz MC, Mortara RA, Roque-Barreira MC, da Silva CV. Recruitment of galectin-3 during cell invasion and intracellular trafficking of *Trypanosoma cruzi* extracellular amastigotes. *Glycobiology.* 2014; 24: 179-184.

20. de Oliveira Filho GB, de Oliveira Cardoso MV, Espíndol JW, Ferreira LF, de Simone CA, Ferreira RS, Coelho PL, Meira CS, Magalhães Moreira DR, Soares B, Lima Leite AC. Structural design, synthesis and pharmacological evaluation of 4-thiazolidinones against *Trypanosoma cruzi*. *Bioorg. Med. Chem.* 2015; 23: 7478-7486.

21. Robledo-O’Ryan N, Matos MJ, Vazquez-Rodriguez S, Santana L, Uriarte E, Moncada-Basualto M, Mura F, Lapier M, Maya JD, Olea-Azar C. Synthesis, antioxidant and antichagasic properties of a selected series of hydroxy-3-arylcoumarins. *Bioorg. Med. Chem.* 2017; 25: 621-632.

22. Silva-Júnior EF, Silva EPS, França PHB, Silva JPN, Barreto EO, Silva EB, Ferreira RS, Gatto CC, Moreira DR, Siqueira-Neto JL, Mendonça-Júnior FJB, Lima MCA, Bortoluzzi JH, Scotti MT, Scotti L, Meneghetti MR, Aquino TM, Araújo-Júnior JX. Design, synthesis, molecular docking and biological evaluation of thiophen-2-iminothiazolidine derivatives for use against *Trypanosoma cruzi*. *Bioorg. Med. Chem.* 2016; 24: 4228-4240.

23. Ogindo CO, Khraiwesh MH, George M, Brandy Y, Brandy N, Gugssa A, Ashraf M, Abbas M, Southerland WM, Lee CM, Bakare O, Fang Y. Novel drug design for Chagas disease via targeting *Trypanosoma cruzi* tubulin: Homology modeling and binding pocket prediction on *Trypanosoma cruzi* tubulin polymerization inhibition by naphthoquinone derivatives. *Bioorg. Med. Chem.* 2016; 24: 3849-3855.

24. Cardoso MF, Salomão K, Bombaça AC, da Rocha DR, da Silva F de C, Cavaleiro JA, de Castro SL, Ferreira VF. Synthesis and anti-*Trypanosoma cruzi* activity of new 3-phenylthio-nor- β -lapachone derivatives. *Bioorg. Med. Chem.* 2015; 23: 4763-4768.

25. da Silva LE, Joussef AC, Pacheco LK, da Silva DG, Steindel M, Rebelo RA. Synthesis and in vitro evaluation of leishmanicidal and trypanocidal activities of N-quinolin-8-yl-arylsulfonamides. *Bioorg. Med. Chem.* 2007; 15: 7553-7560.

26. Pagliero RJ, Lusvarghi S, Pierini AB, Brun R, Mazzieri MR. Synthesis, stereoelectronic characterization and antiparasitic activity of new 1-benzenesulfonyl-2-methyl-1,2,3,4-

tetrahydroquinolines. *Bioorg. Med. Chem.* 2010; 18: 142-150.

27. Kim JH, Ryu HW, Shim JH, Park KH, Withers SG. Development of new and selective *Trypanosoma cruzi* trans-sialidase inhibitors from sulfonamide chalcones and their derivatives. *ChemBioChem.* 2009; 10: 2475-2479.

28. Junqueira G, Carvalho MR, Andrade P, Lopes CD, Carneiro ZA, Sesti-Costa R, Silva JS, Carvalho I. Synthesis and in vitro evaluation of novel galactosyl-triazolo-benzenesulfonamides against *Trypanosoma cruzi*. *J. Braz. Chem. Soc.* 2014; 25: 1872-1884.

29. Marchiori MF, Souto DE, Pereira JF, Kubota LT, Cummings RD, Dias-Baruffi M, Carvalho I, Campo VL. Synthetic 1,2,3-triazole-linked glycoconjugates bind with high affinity to human galectin-3. *Bioorg. Med. Chem.* 2015; 23: 3414-3425.

30. Campo VL, Sesti-Costa R, Carneiro ZA, Silva JS, Schenkman S, Carvalho I. Design, synthesis and the effect of 1,2,3-triazole sialylmimetic neoglycoconjugates on *Trypanosoma cruzi* and its cell surface trans-sialidase. *Bioorg. Med. Chem.* 2012; 20: 145-156.

31. Bräse S, Gil C, Knepper K, Zimmermann V, Organic azides: an exploding diversity of a unique class of compounds. *Angew. Chem., Int. Ed.* 2005; 44: 5188-5240.

32. Mori K. Synthesis and absolute configuration of (–)-ipsenol (2-methyl-6-methylene-7-octen-4-ol), the pheromone of ipsaraconfusus lanier. *Tetrahedron Lett.* 1975; 16: 2187-2190.

33. Aragao-Leoneti V, Campo VL, Gomes AS, Field RA, Carvalho I. Application of copper (I)-catalysed azide/alkyne cycloaddition (CuAAC) 'click chemistry' in carbohydrate drug and neoglycopolymer synthesis. *Tetrahedron.* 2010; 66: 9475-9492.

34. Campo VL, Riul TB, Carvalho I, Baruffi MD. Antibodies against mucin-based glycopeptides affect *Trypanosoma cruzi* cell invasion and tumor cell viability. *ChemBioChem.* 2014; 15: 1495-1507.

35. Chaussabel D, Jacobs F, de Jonge J, de Veerman M, Carlier Y, Thielemans K, Goldman M, Vray B. CD40 ligation prevents *Trypanosoma cruzi* infection through interleukin-12 upregulation. *Infect Immun.* 1999; 67:1929-34.

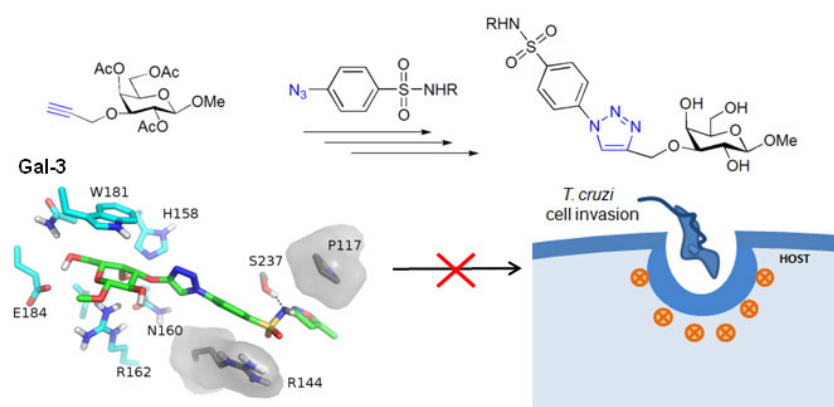
36. Rolón M, Vega C, Escario JA, Gómez-Barrio A. Development of resazurin microtiter assay for drug testing of *Trypanosoma cruzi* epimastigotes. *Parasitol Res.* 2006; 99: 103–107.

37. Neres J, Buschiazzi A, Alzari PM, Walsh L, Douglas KT. Continuous fluorimetric assay for high-throughput screening of inhibitors of trans-sialidase from *Trypanosoma cruzi*. *Anal. Biochem.* 2006; 357: 302-304.

38. Neres J, Bonnet P, Edwards PN, Kotian PL, Buschiazzi A, Alzari PM, Bryce RA, Douglas KT. Benzoic acid and pyridine derivatives as inhibitors of *Trypanosoma cruzi* trans-sialidase. *Bioorg. Med. Chem.* 2007; 15: 2106-2119.

39. Stowell SR, Arthur CM, Mehta P, Slanina KA, Blixt O, Leffler H, Smith DF, Cummings RD. Galectin-1, -2, and -3 exhibit differential recognition of sialylated glycans and blood group antigens. *J Biol Chem.* 2008; 283:10109-10123.

40. Farina B, Di Sorbo G, Chambery A, Caporale A, Leoni G, Russo R, Mascanzoni F, Raimondo D, Fattorusso R, Ruvo M, Doti N. Structural and biochemical insights of Cyp A and AIF interaction. *Sci. Rep.* 2017; 7: 1138.
41. Miller III BR, McGee Jr TD, Swails JM, Homeyer N, Gohlke H, Roitberg AE. MMPBSA.py: an efficient program for end-state free energy calculations. *J. Chem. Theory Comput.* 2012; 8: 3314-3321.
42. Van Der Spoel D, Lindahl E, Hess B, Groenhof G, Mark AE, Berendsen HJ. GROMACS: fast, flexible, and free. *J. Comput. Chem.* 2005; 26: 1701-1718.
43. Schenkman S, Chaves LB, de Carvalho LCP, Eichinger DJ. A proteolytic fragment of *Trypanosoma cruzi* trans-sialidase lacking the carboxyl-terminal domain is active, monomeric, and generates antibodies that inhibit enzymatic activity. *Biol. Chem.* 1994; 269: 7970-7975.
44. Rocha GB, Freire RO, Simas AM, Stewart JJ. RM1: A reparameterization of AM1 for H, C, N, O, P, S, F, Cl, Br, and I. *J. Comput. Chem.* 2006; 27: 1101-1111.
45. Stewart JJ. MOPAC: a semiempirical molecular orbital program. *J. Comput. Aided Mol. Des.* 1990; 4: 1-103.
46. Wang J, Wang W, Kollman PA, Case DA. Automatic atom type and bond type perception in molecular mechanical calculations. *J. Mol. Graph. Model.* 2006; 25: 247-260.
47. Sörme P, Arnoux P, Kahl-Knutsson B, Leffler H, Rini JM, Nilsson UJ. Structural and thermodynamic studies on cation- π interactions in lectin-ligand complexes: high-affinity galectin-3 inhibitors through fine-tuning of an arginine-arene interaction. *J. Am. Chem. Soc.* 2005; 127: 1737-1743.
48. Lindorff-Larsen K, Piana S, Palmo K, Maragakis P, Klepeis JL, Dror RO, Shaw, DE. Improved side-chain torsion potentials for the Amber ff99SB protein force field. *Proteins: Struct., Funct., Bioinf.* 2010, 78: 1950-1958.
49. Wang J, Wolf RM, Caldwell JW, Kollman PA, Case DA. Development and testing of a general amber force field. *J. Comp Chem.* 2004; 25: 1157-1174.



ACCEPTED